The author wishes to thank Dr. A. H. Silver of this laboratory for his enlightening discussions of this work.

[1] Wyckoff, R. W. G., *Crystal Structure*, (New York: Interscience Publishers, 1951), chap. 8 p. 9.

[2] Bennett, J. E., and D. J. E. Ingram, *Phil. Mag.*, **1**, 109 (1956).

[3] Bennett, J. E., D. J. E. Ingram, and D. Schonland, *Proc. Phys. Soc.* (*London*) **A69**, 556 (1956).

---

*CONTINUOUS ELECTROPHORETIC FRACTIONATION STABILIZED BY ELECTROMAGNETIC ROTATION**

BY ALEXANDER KOLIN

DEPARTMENT OF BIOPHYSICS, UNIVERSITY OF CALIFORNIA, LOS ANGELES

Communicated by Walter M. Elsasser, February 8, 1960

The objective of the experiments described below is to achieve continuous separation of ions in solution by making charged particles of different mobilities follow divergent paths. Similar aims have been pursued by other authors employing different means. Grassman and Hannig[1] utilized in their paper curtain electrophoresis gravitational descent of a flowing zone of the dissolved mixture of ions along a curtain of filter paper in a transverse electric field. Svensson and Brattsten[2] aimed to achieve the same result by using glass powder as a medium to suppress thermal convection. Mel[3] used a density gradient for stabilization, putting gradient zone electrophoresis[4,5] on a continuous flow basis, and Dobry and Finn[6] relied on suppression of thermal convection in a viscous vertical flow column. The present approach differs from the previous ones in that no porous media or concentration gradients are required for stabilization against thermal convection, and in the use of electromagnetic forces in combination with an electric field to obtain the desired motion of the ions in a free solution, stabilization being achieved by revolution of the electrophoretic column about a horizontal axis. The resulting stability is so great that high current densities in cooled liquid columns can be employed permitting continuous application of potential gradients in the vicinity of 50 Volts/cm and brief application of fields exceeding 100 Volts/cm. The use of very thin and sharp "streaks" of ions in strong electric fields leads to clear-cut separations within time intervals of the order of a few seconds (Fig. 10*d*). The method is applicable to suspended particles as well as to ions in solution.

The application described below is designed for separation on a micro-scale, processing mixtures at the rate of less than 0.01 cc/min. No attempt has been made as yet to construct an apparatus for large-scale separations.

Principle of the Method.—The main experimental difficulty to be overcome is thermal convection. In addition to the above mentioned methods of stabilization,[1-6] there are two stabilization principles which have not been used as yet for continuous flow separations: (*a*) Stabilization by an electromagnetic force field,[7] which has been used so far only in experiments on electromagnetophoresis, and (*b*) stabilization by rotation of the fluid[8,9] which has been used practically so far only with zone electro-

phoresis in free solution.[9] The latter method (*b*) is based on the following consideration. A heated fluid element which tends to rise in the field of gravity due to diminution of its density below that of the surrounding fluid will describe a circular motion instead of rising steadily, if the cell is rotated slowly. As a result, thermal convection does not develop even in the presence of high local density gradients of thermal origin.[8] This principle is utilized in the present method. A horizontal cylindrical fluid column of annular cross-section is maintained in rotation about its axis of symmetry by electromagnetic forces which inhibits thermal convection.

The rotation of the fluid column is produced by a combination of a longitudinal electric current with a radial magnetic field, as shown in Figure 1. The $\mathbf{B}_r$ vectors represent radial components of the magnetic field in a plane perpendicular to the axis of the bar magnet (M) at a distance R from the magnet axis. **J** represents the vector of current density in the conductive fluid surrounding the magnet and $\mathbf{f} = [\mathbf{J} \times \mathbf{B}]$ the force density, i.e., the force exerted upon each unit volume element

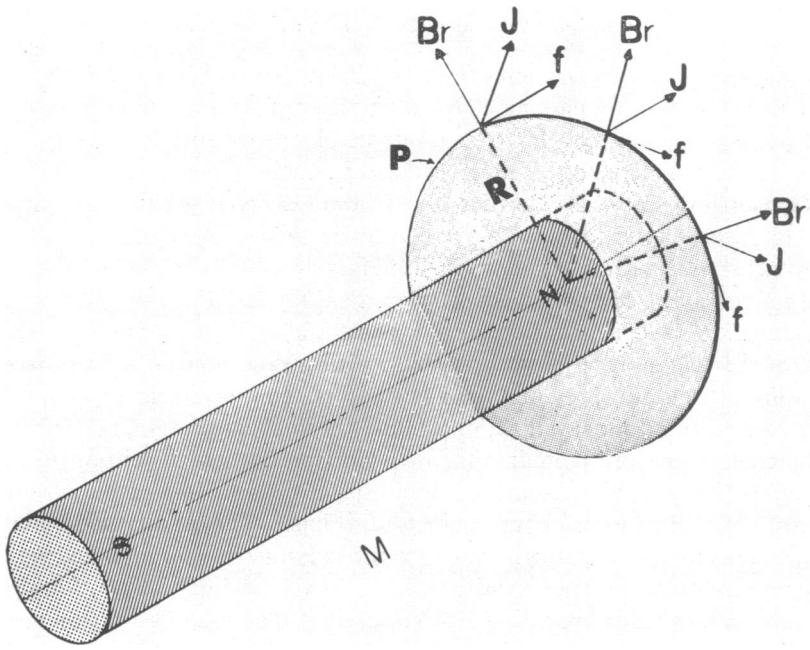

FIG. 1.—Spatial configuration of the vectors $\mathbf{B}_r$, **J**, and **f**. *N*, *S*: poles of the bar magnet.

at right angles to $\mathbf{B}_r$ and **J**. The circular arc P represents a path of a fluid element. Fluid particles along the periphery P will be set in rotation about the bar magnet by electromagnetic forces. In order to obtain a radial magnetic field of adequate longitudinal extent and uniformity, the opposing like poles of two bar magnets M_1 and M_2 can be bridged by an intermediate short, soft iron cylinder *m* as shown in Figures 2, 3*a*, and 7*b*. The resulting distribution of the radial component of the magnetic field intensity at the distance R from the axis is indicated in Figure 7 for a single bar magnet and for the arrangement of two bar magnets described above. The field intensity distribution was determined by means of a mercury jet magnetometer[10]

by moving the magnet past the magnetometer and recording directly the radial component of the magnetic field.

The electrophoretic column is made short enough to be penetrated only by a small section of the magnetic field of adequate radial intensity (namely, the section adjacent to the magnet poles), as shown in Figure 2. This perspective view shows an electrophoretic cell consisting of three externally discernible sections. B is the annular electrophoretic column surrounding the central channel into which the ends of

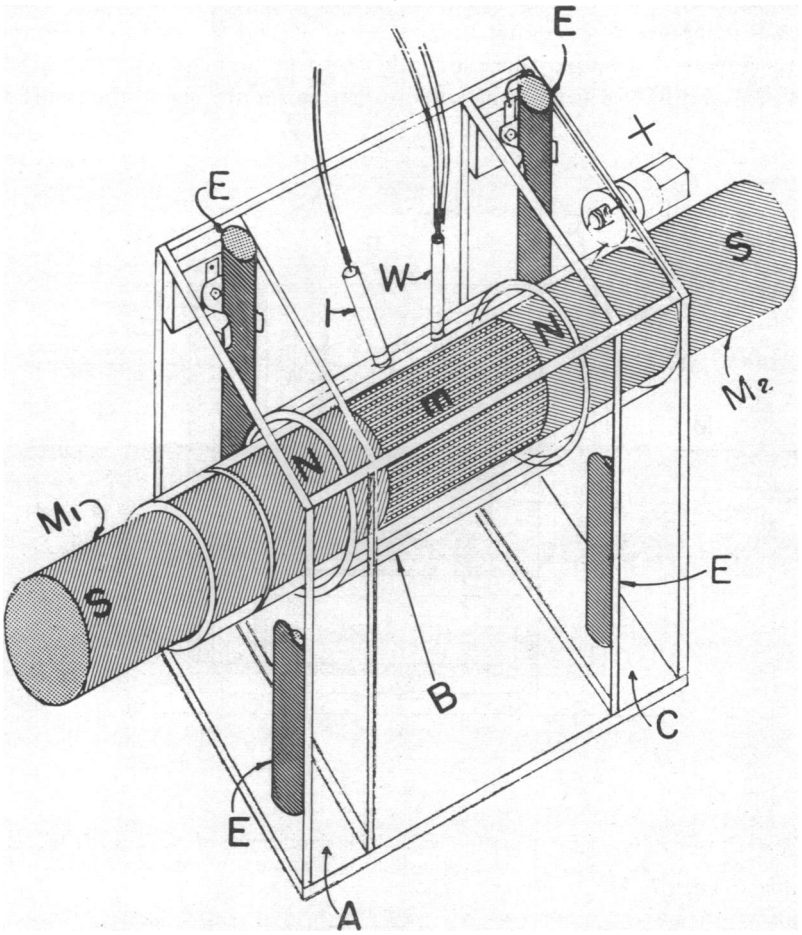

FIG. 2.—Perspective view of the fractionation cell. *N, S:* poles of the bar magnets M_1 and M_2; *m:* soft iron spacer; *E:* four graphite electrodes (the two front electrodes are shown only partly). Each electrode compartment (*A* and *C*) harbors two electrodes which are connected to a common binding post. Only the positive binding post is shown. *I:* injector from which the mixture to be fractionated enters the cell; *W:* withdrawal peg through which separated fractions are removed; *B:* the actual fractionation space surrounded by lucite walls. The tub thus formed is filled with an ice-water mixture.

the bar magnets M_1 and M_2 are inserted. *m* is the soft iron section sandwiched between the end faces of the cylindrical bar magnets M_1 and M_2. A and C are electrode compartments which are communicating with the ends of the annular electrophoretic column, and E represents graphite rod electrodes. The bottom and

the sides of the electrode compartments are bridged by lucite plates so as to create a transparent bath surrounding the section B. This bath is filled with ice-water mixture to cool the electrophoretic column. The latter is thus an annular cylindrical volume bounded on the inside by a lucite cylinder surrounding the bar magnets and on the outside by a cylinder in contact with the ice-water bath. The width of the annulus is 1.5 mm and its axial length is 6 cm. The thickness of the cylinder walls is 0.5 mm.

Figure 3 shows the cell design in greater detail. Figure 3*a* is a central longitudinal cut showing the electrode compartments A and C and the annular electrophoretic column segment B between them, bounded by the lucite tubes IT and ET. The magnets M_1 and M_2 as well as the soft iron spacer *m* are inside the lucite tube IT.

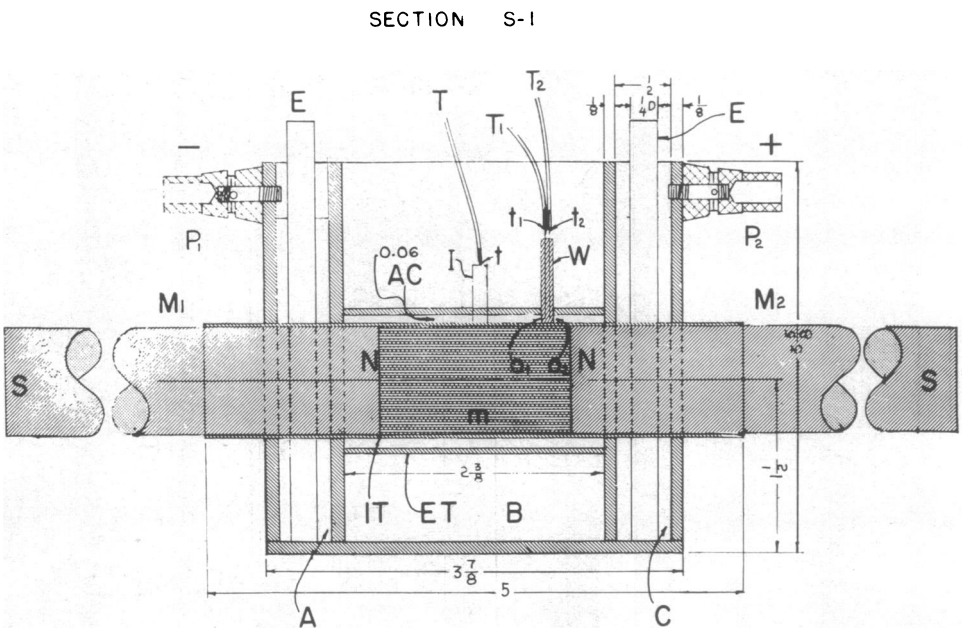

FIG. 3*a*.—Cross-section of fractionation cell. The significance of *N*, *S*, *m*, *I*, *W*, *A*, *C*, *B*, and *E* is the same as in Fig. 2. P_1P_2: binding posts; *AC:* annular electrophoretic channel; *t*, t_1, t_2: hypodermic tubing; *T*, T_1, T_2: plastic tubing.

W is a teflon rod (shown magnified for greater detail in Fig. 3*b*) provided with the two openings 0_1 and 0_2 which serve for withdrawal of separated fractions. These openings communicate through the metal tubes t_1 and t_2 with the plastic tubes T_1 and T_2 which lead to the fraction collectors. The line O_1 O_2 is parallel to the magnet axis. Section S_2 shown in Figure 3*c* is taken through the center of the cell. It shows the iron core *m* and the lucite tubes IT and ET which enclose the annular space AC between them. The teflon insert I (shown in detail in Fig. 3*d*) serves the purpose of introducing the ion mixture to be fractionated. The injection channel I terminating in opening H is aligned parallel to the magnet axis. The metal tube *t* communicates through the plastic tubing T with the reservoir of the solution to be fractionated. Section S_2 shown in Figure 3*c* indicates the placement of the graphite

electrodes E relative to the annular aperture AC of the electrophoretic column. Circular graphite electrodes in the shape of rings surrounding the annular aperture AC are preferable to rod electrodes for mobility measurements to avoid distortion of the ion path, which becomes apparent in the vicinity of the electrode compartments; but for fractionation purposes, the rod electrodes are adequate.

Mode of Operation.—A longitudinal electric current is passed through the annular liquid column in section B by application of a potential difference to the electrodes in the compartments A and C. Due to interaction of this current with the radial component of the magnetic field permeating the annular space AC, the fluid in the annular column is set in rotation. We shall make the initial simplifying assumption that the speed of the fluid is everywhere the same in the annular space. The solution to be fractionated is expelled slowly through the aperture H of insert I by action of gravity from a raised reservoir connected to the hypodermic tubing *t* through a polyethylene tube T (Figs. 3*c* and 3*d*). By choosing a small enough aperture H (0.25 mm), a very fine "streak" of solution is injected into the annular space midway between the walls IT and ET. Due to the longitudinal electric field concomitant with the current passing between the electrode compartments A and C, the ions in the "streak" migrate parallel to the magnet axis with speeds determined by their mobilities and by the potential gradient. The ion path is thus a spiral. The pitch of the spiral is a function of the ion mobility, the longitudinal potential gradient, and the angular velocity of the rotating fluid. Since both the longitudinal velocity of the ions and the angular velocity of the fluid column are proportional to the voltage applied to the cell, the pitch of the spiral ionic path should be independent of the cell voltage, so that voltage fluctuations would not affect the sharpness of the spiral "streaks". This independence has actually been demonstrated experimentally (see below).

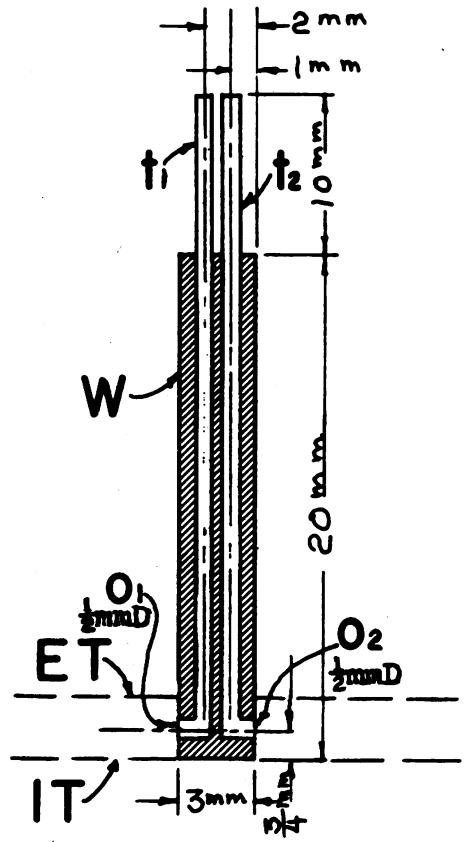

FIG. 3*b*.—*W*: Withdrawal peg. *ET* and *IT*: external and internal boundary, respectively, of the annular electrophoresis channel; O_1, O_2: openings of the withdrawal channels; t_1, t_2: hypodermic tubing.

The approximate magnitude of the pitch to be expected can be calculated as follows taking into account the non-uniformity of the velocity distribution in the annulus. For an annulus whose width is small compared to its mean radius of curvature, the rotary flow of the fluid can be treated, according to Lamb, approximately as a viscous flow between straight parallel plates.[11] Figure 4 shows a trans-

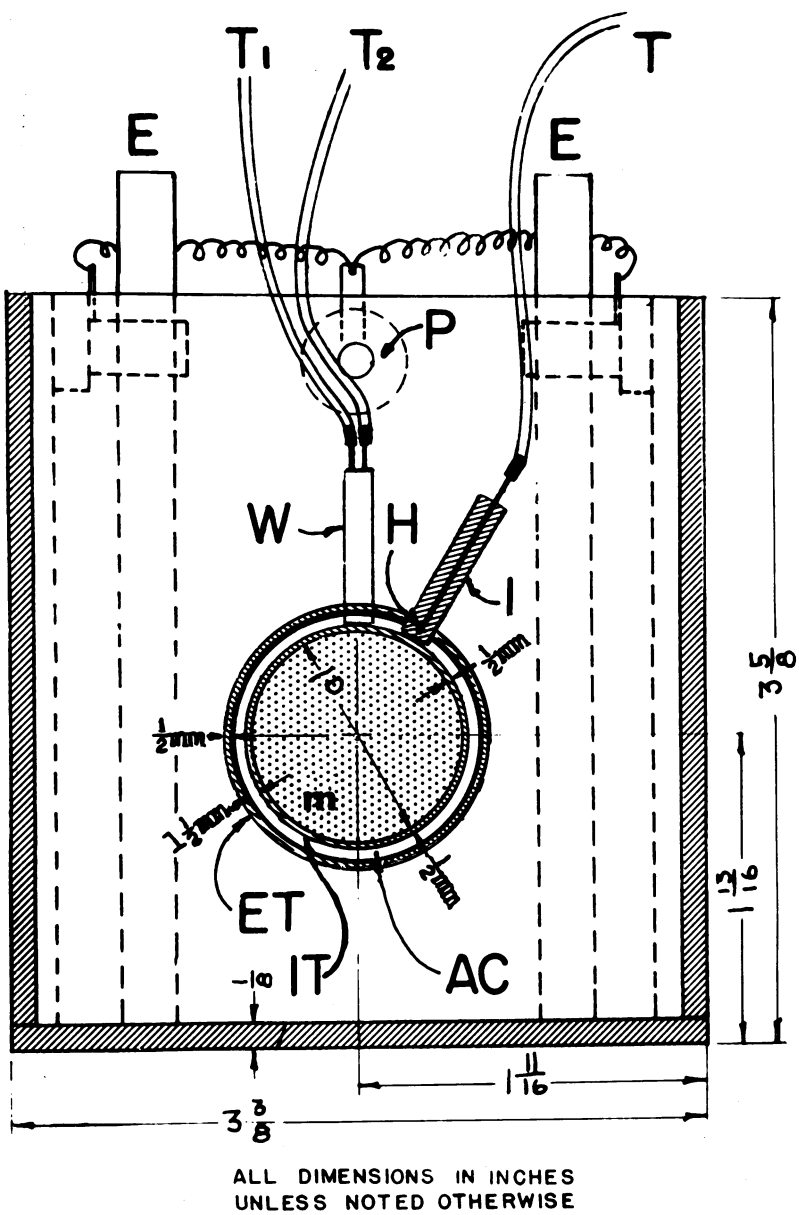

FIG. 3c.—Section through center of the cell. The meaning of *m*, *E*, *P*, *T*, T_1, T_2, *IT*, *ET*, *AC*, *I*, and *W* is the same as in Figs. 2 and 3*a*. *H:* opening through which the solution to be fractionated is injected into the space *AC*.

verse section through the annular tube. The inner radius of the annulus is R and the outer one R + h. The distance of an arbitrary point from the cylinder axis is *r*.

The local tangential velocity u at radial distance r due to rotary motion of the fluid in the annulus is given by

$$u = (1/2\eta)z(z-h)(dp/dx) \tag{1}$$

where $z = (r - R)$ and dp/dx is the tangential pressure gradient.[11]

The maximum velocity at the center of the annulus is obtained by setting $z = h/2$:

$$u_0 = -(h^2/8\eta)(dp/dx). \tag{2}$$

The value of dp/dx can be determined from the current density $\mathbf{J}$ and magnetic flux density $\mathbf{B}$;

$$-dp/dx = \mathbf{f} = (1/10)[\mathbf{J} \times \mathbf{B}], \tag{3}$$

where $\mathbf{f}$ is given in dynes/cm^3 if $\mathbf{J}$ is measured in amp/cm^2 and $\mathbf{B}$ in gauss. We obtain thus from (2) and (3):

$$u_0 = (h^2/80\eta)[\mathbf{J} \times \mathbf{B}]. \tag{4}$$

Let us now assume that we inject a very thin "streak" of ions at the center of the annulus so that we can confine our consideration to the central maximum velocity u_0. The pitch of the spiral path described by an ion travelling midway between the walls of the annulus is then simply equal to the longitudinal displacement s_0 of the ion during the time required for a complete revolution of the ion about the cylinder axis. The period of revolution τ_0 for the central fluid layer can be calculated simply from (2):

$$\tau_0 = 2\pi/\omega_0 = (1/u_0)2\pi(R + h/2) \cong 2\pi R/u_0. \tag{5}$$

From (4) and (5) follows:

$$\tau_0 = \frac{160\ \eta\pi R}{h^2\ J\ B}. \tag{6}$$

The pitch s_0 is then given by the displacement of the ion:

$$s_0 = v\tau_0 = (d\phi/dy)U\tau_0 = (d\phi/dy)U(160\ \eta\pi R/h^2JB) \tag{7}$$

where the ion velocity $v = (d\phi/dy)U$ is expressed as a product of the ion mobility U and the longitudinal potential gradient $d\phi/dy$. Expressing

$$d\phi/dy = J/\sigma \tag{8}$$

in equation (7) in terms of current density J and the conductivity σ of the solution, we obtain $s_0 = (J/\sigma)U(160\ \eta\pi R)/(h^2/JB)$. Thus,

$$s_0 = 160\ \eta\pi R/h^2\ (U/B\sigma) = (K/B)(U/\sigma). \tag{9}$$

The current density cancels out and the pitch of the spiral ionic path is seen to depend on the constant K, which is determined by the geometry of the cell as well as the viscosity of the fluid, and on the magnetic and electric parameters B, U and σ.

The ion mobility U is thus determined from equation (9) without resort to time measurement:

$$U = B\sigma s_0/K = G\sigma s_0. \qquad (9a)$$

If the factor G = B/K is kept constant, determination of U involves measurement of a conductivity σ and of a displacement s_0. The measurement of U actually amounts to a comparison between the longitudinal velocity acquired by the ions in the electric field $d\phi/dy$ with the tangential velocity imparted to them by the rotation of the fluid column.

The following numerical example illustrates the order of magnitude of the effect. Assume the following data:

$$J = 10^{-2}\ \text{amp/cm}^2;\ h = 0.16\ \text{cm};\ B = 150\ \text{gauss};\ R = 1.5\ \text{cm};$$
$$U = 10^{-4}\ \text{cm/sec/(Volt/cm)};\ d\phi/dy = 50\ \text{Volts/cm};\ \eta = 10^{-2}\ \text{poise}.$$

From (7) follows:

$$s_0 = 50 \cdot 10^{-4}\ (1.6\ \pi\ 1.5)/(2.56 \cdot 10^{-2} \cdot 10^{-2} \cdot 150) \cong 1\ \text{cm}.$$

Effects of the Velocity Distribution and Electro-Osmosis.—In the preceding treatment, the velocity distribution in the rotating fluid was assumed to be parabolic, with the local velocity given by equation (1). This is actually a simplified picture which is correct only in the absence of electro-osmotic streaming. In general, the streaming pattern in the annular fluid column will be complicated by electro-osmotic convection. Due to charge separation at the interface between the electrolyte and the cell wall (ionic double layer) the charged electrolyte layer near the wall is set in motion toward the electrode of opposite polarity. In a closed system, this flow is balanced by a flow in opposite direction at the center of the cell so that the net transfer of fluid through the cell is zero. Figure 5 shows the resulting distribution of longitudinal velocity in a cell of rectangular cross-section whose width h is negligible compared to its depth (measured at right angles to the plane of the paper). This phenomenon has been studied by Smoluchowski,[12] who showed that the velocity distribution in electro-

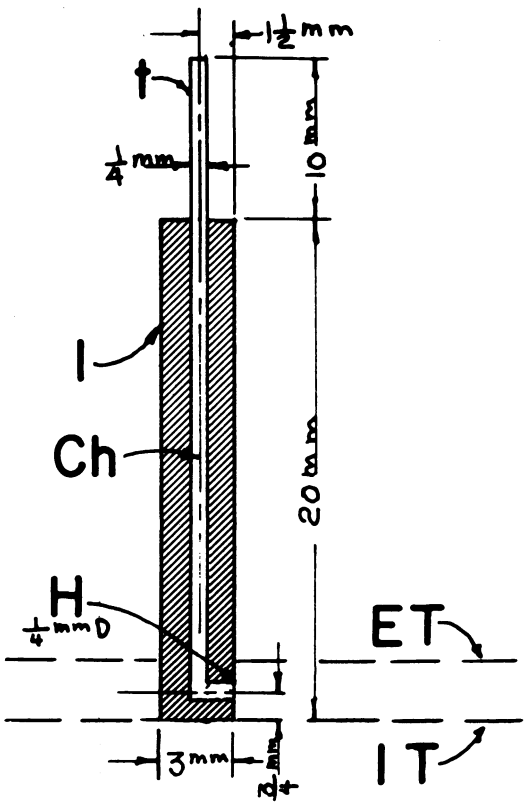

FIG. 3*d*.—I: injection peg; *Ch:* injection channel; *H:* opening through which solution to be fractionated enters the space *AC* bounded by the walls *IT* and *ET;* t: hypodermic tubing.

osmotic streaming is parabolic. The fluid moves in opposite directions at the center and near the cell walls. Two zones (Z_1 and Z_2 of Fig. 5) of zero velocity separate the oppositely directed streams of fluid. The location of these zones is independent of the cell depth h and of the velocity of electro-osmotic streaming.

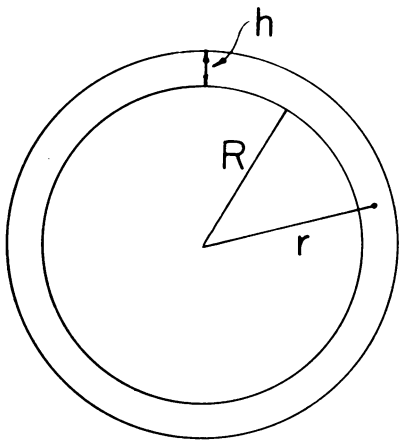

FIG. 4.—See text.

In our annular electrophoresis cell, the electro-osmotic streaming is parallel to the cylinder axis, whereas the electromagnetically engendered circulation is at right angles to it. The velocity distribution is approximately parabolic for both fluid movements. Both, the longitudinal velocity due to electro-osmotic streaming (referred to below for brevity as "longitudinal velocity") and the transverse velocity due to rotation of the annular fluid column (referred to below for brevity as "transverse velocity"), are largest at the center of the annulus and both diminish in parabolic fashion with distance from the center. The fluid elements describe thus a spiral path winding about the axis of the annular cylinder. If both the longitudinal and the transverse velocity distributions were of the form given by equation (1), the pitch of the resulting spiral, which is determined by the ratio between these two velocities, would be constant over the entire width h of the annulus. Actually, as will be shown below, this is not the case. The fluid particles in the zones of zero longitudinal velocity† describe circular paths, whereas the fluid elements beyond these zones move along spirals. If the fluid particles within the space between the cylindrical zones of zero longitudinal velocity describe a right-handed spiral, those outside this space move on left-handed spirals.

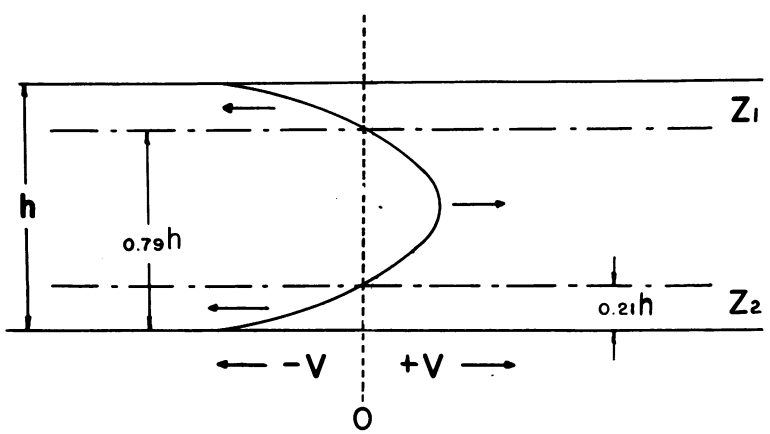

FIG. 5.—Velocity distribution between parallel planes (perpendicular to the page) due to electro-osmotic streaming. The applied electric field is parallel to the arrows. The arrows indicate the direction of flow. Z_1, Z_2: zones of zero velocity (parallel to the walls). h: distance between the parallel planes.

The electrophoretic migration of ions injected into this streaming pattern is superimposed upon the fluid movement caused by the combination of electro-osmotic and electromagnetically engendered convection. The local transverse velocity u of the fluid and the entrained ions is given by equation (1) $u = (1/2\eta)(dp/dx)z(z - h)$. The longitudinal velocity v^* results from two effects: (1) electrophoretic migration and (2) transport due to electro-osmotic streaming.[13] The spatial correlation between the axes u, v, and z is shown in Figure 6. The expression for the electro-osmotic streaming velocity v is very similar to equation (1) giving the transverse velocity u as a function of distance from the cell wall. We obtain v from the differential equation expressing the viscous drag force in terms of the pressure gradient:[13]

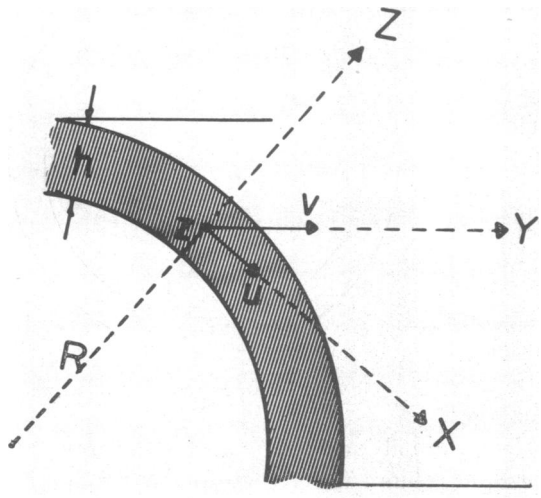

FIG. 6.—See text.

$$dp/dy = \eta(d^2v/dz^2). \tag{10}$$

Integration of equation (10) yields:

$$v = (1/2\eta)z^2(dp/dy) + Az + B. \tag{11}$$

The values of A and B can be found from the boundary condition specifying the magnitude of electro-osmotic streaming velocity V at the walls (i. e., at $z = O$ and $z = h$). Setting $z = O$ we get $B = V$. And setting $z = h$ we obtain: $V = (1/2\eta)h^2(dp/dy) + Ah + V$. Thus, $A = -(1/2\eta)h(dp/dy)$ and

$$v = (1/2\eta)(dp/dy)z(z - h) + V. \tag{12}$$

The main difference between equations (1) and (12) is the term V of equation (12) which expresses the fact that the electro-osmotic longitudinal velocity v does not vanish at the cell walls.

The longitudinal velocity v^* of an ion of mobility U is obtained by superposition of the ion velocity relative to the electrolyte upon the electrolyte velocity v relative to the cell:

$$v^* = (1/2\eta)(dp/dy)z(z - h) + E(W - U). \tag{13}$$

The electro-osmotic streaming velocity $V = EW$ has been expressed in equation (13) as a product of the electric field intensity E and the streaming velocity W engendered in a field of unit intensity.

The pitch of an ionic spiral path at any distance from the cell wall is obtained as the longitudinal displacement s during the period of revolution τ of the ion about the magnet axis. Since $\tau \cong 2\pi R/u$ (comp. equation (5)), we get, taking equations (1)

and (13) into consideration and setting u = EC (C being the value of u at unit field strength):

$$s = v^*\tau = 2\pi R v^*/u = 2\pi R\left[\frac{(1/2\eta)(dp/dy)z(z-h)}{(1/2\eta)(dp/dx)z(z-h)} + \frac{E(W-U)}{EC}\right] \quad (14)$$

or

$$s = 2\pi R\left[\frac{dp}{dy}\Big/\frac{dp}{dx} + (W-U)/C\right]. \quad (14a)$$

Due to dependence of C on distance from the wall, the pitch s will be constant over the entire width h of the annulus only for the case W = U. In general, a spiral ion path of sufficiently constant pitch can be obtained for any value of W − U by confining the ions to a narrow zone about the center of the annulus where C varies but slightly in conformity with the parabolic velocity distribution. Accordingly, the experiments described below were performed with thin streaks of ions injected at the center of the annulus.

Experimental Illustrations.—Figure 7 shows spiral streaks obtained with a single ion species India ink. In Figure 7*a*, the non-uniformity of the radial magnetic field near one end of a bar magnet accounts for the variation in the pitch of the spiral. The distribution of the radial magentic field intensity component (recorded by means of a mercury jet magnetometer[10]) is shown above the photograph of the spiral streaks and the diagram of the magnet in Figure 7*a*. In Figure 7*b*, a soft iron cylinder *m* is interposed between the magnet poles. The result is a zone of fairly uniform intensity of the radial magnetic field component, which accounts for the nearly constant pitch of the spiral. The absolute value of the magnetic field was ascertained by means of a mercury jet magnetometer.

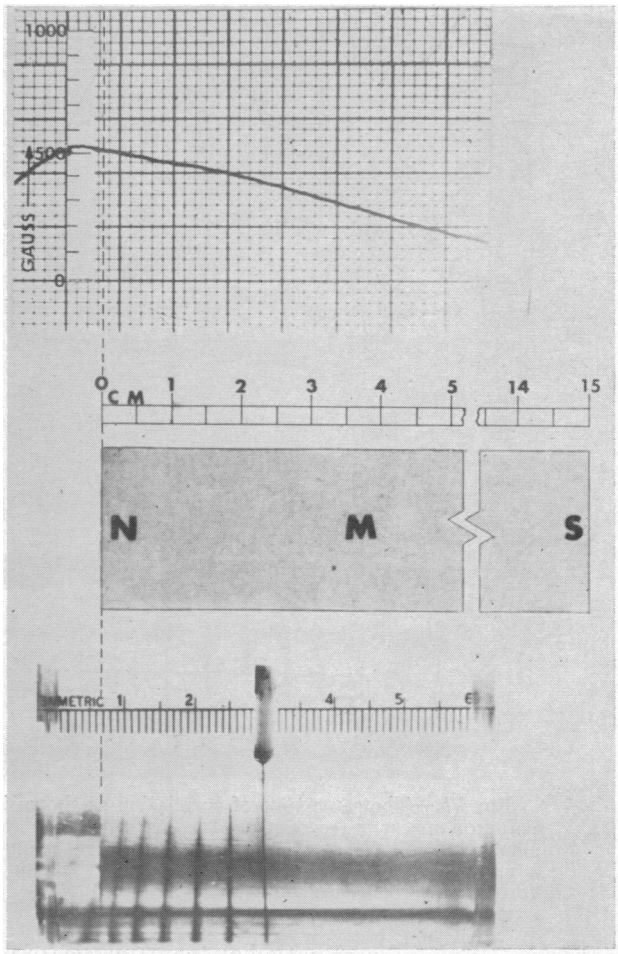

FIG. 7*a*.—Correlation between the magnetic field intensity distribution (top graph) and the pitch of the spiral ion path (bottom photograph) for a single bar magnet (bottom photograph and drawing marked by letters *N*, *M*, *S*).

Figure 8 shows fractionation of the dyes *Evans blue* and *rose bengal* in a dilute pH 5 buffer (obtained by dissolving one pH 5 "Hydrion" buffer tablet in 1 liter of water). After several turns of the spiral, some of the separated fractions may overlap, such as, for instance, *rose bengal* and *Evans blue* in the second streak from the left in Figure 8. The picture is reminiscent of spectral lines of different color obtained with diffraction gratings yielding several orders of interference. The use of several spiral turns is of advantage in separating ions differing but little in mobility.

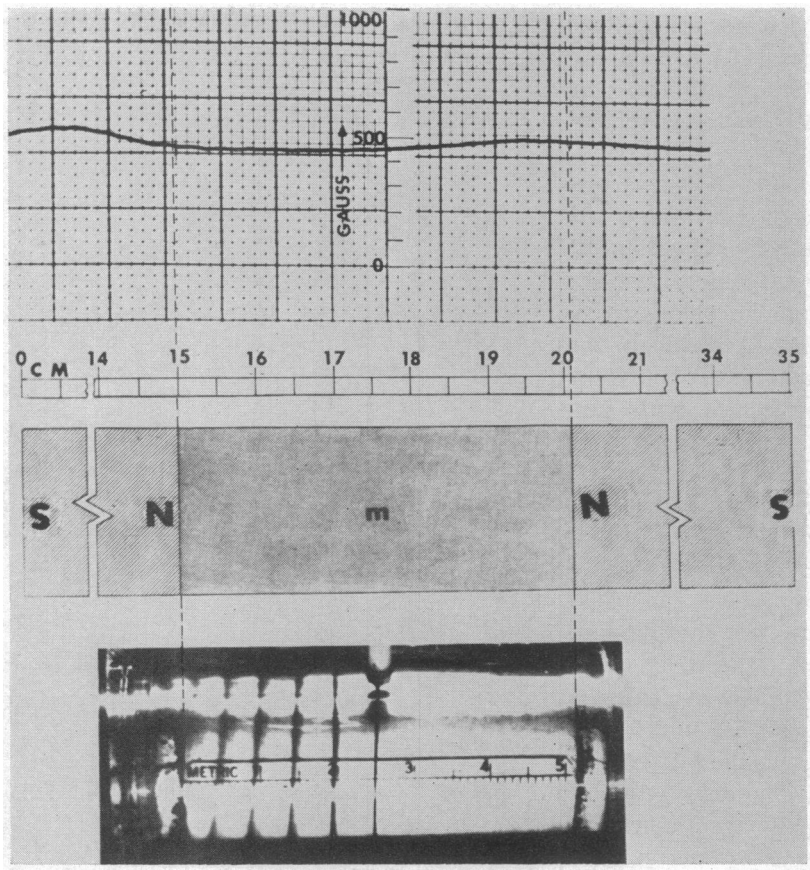

FIG. 7*b*.—The same type of correlation as shown in Fig. 7*a* for the case of a soft iron spacer *m* (see central drawing marked by *S, N, m, N, S*) between two like poles (*N, N*) of two bar magnets. The magnetic field distribution (top graph) and the distribution of spiral pitch (bottom photograph) are more uniform than for the case shown in Fig. 7*a*.

Figure 9 depicts fractionation of 3 ionic species of like charge using a higher spiral pitch than the preceding fractionation. This separation of a mixture of *India ink, rose bengal,* and *Evans blue* is carried out in a dilute pH 7 buffer (obtained by dissolving one pH 7 "Hydrion" buffer tablet in 2 liters of water).

Figure 10 illustrates the effects of variation in voltage across the electrophoresis cell and of variation in the electrical conductivity of the buffer. The spiral of the *Evans blue* ions in Figure 10*a* has been obtained by application of a voltage of 75

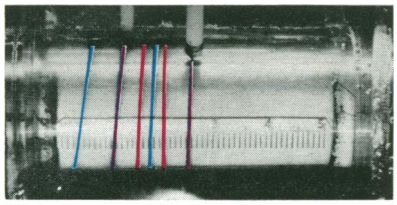

Fig. 8

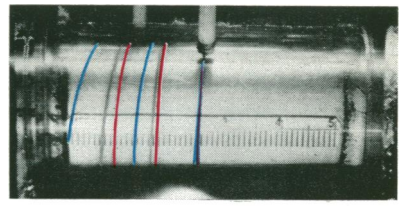

Fig. 9

FIG. 8.—Separation of *rose bengal* from *Evans blue*. The sequence of lines seen from right to left is: (1) initial unresolved streak, (2) rose bengal, (3) Evans blue, (4) rose bengal, (5) overlapping of rose bengal and Evans blue, (6) Evans blue.

FIG. 9.—Separation of a mixture of *India ink*, *rose bengal*, and *Evans blue*. The sequence of lines seen from right to left is: (1) initial streak in beginning stage of separation, (2) rose bengal, (3) India ink, (4) Evans blue, (5) rose bengal, (6) India ink, (7) Evans blue.

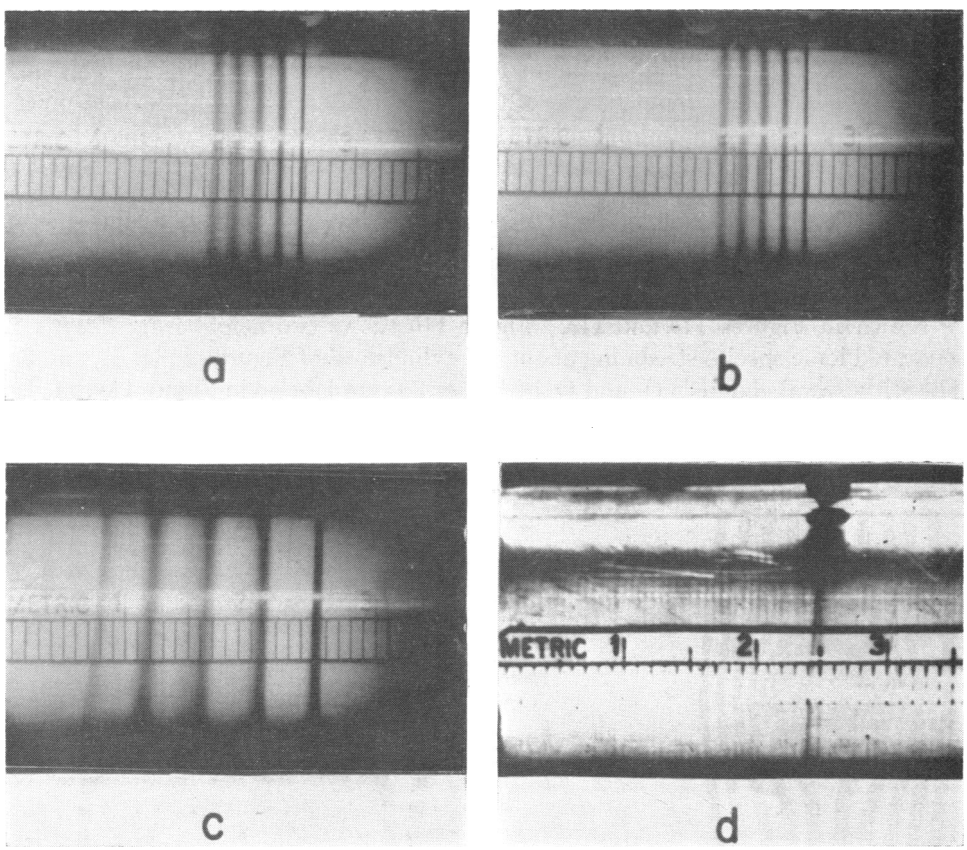

FIGS. 10*a*, *b*, *c*.—Effect of cell voltage on the pitch of the spiral. (*a*) Spiral of Evans blue obtained at a cell voltage of 75 volts and cell current of 25 mA. (*b*) Spiral of Evans blue obtained in the same buffer after doubling the cell current and voltage.

Effect of buffer conductivity on the pitch of spiral. (*c*) Spiral of Evans blue obtained at the same current as used in experiment (*a*) after diluting the buffer 1:2.

FIG. 10*d*.—Illustration of separation speed. Separation of rose bengal from Evans blue achieved within approximately 4 sec at a cell voltage of 700 volts.

volts containing pH 7 "Hydrion" buffer (2 buffer tablets per liter of water) at a current of 25 mA. In Figure 10*a* the appearance of the *Evans blue* spiral after doubling the current and voltage is shown. No appreciable change in the pitch of the spiral has been produced.

In Figure 10*c* we see a spiral obtained with the same ionic species in a pH 7 buffer prepared by 1:2 dilution of the buffer used in the experiment illustrated in Figure 10*a* at the same current strength of 25 mA. The pitch of the ionic spiral thus obtained is somewhat more than twice as large as the pitch of the spiral seen in Figure 10*a*.

The speed with which separations of ionic species can be achieved is illustrated by Figure 10*d* which shows a streak containing a mixture of *Evans blue* and *rose bengal* split into two components approximately 4 sec. after injection of the mixture into the fractionation column (pH 5 "Hydrion" buffer; $^1/_2$ buffer tablet per liter of solution; voltage across the cell: 700 Volts).

Having resolved the original mixture of ions into separate components, it is necessary to remove the individual components into separate containers. For adequate resolution, it is desirable to devise a method of withdrawal of separated ion "streaks" which are no more than a few tenths of a millimeter apart. This cannot be accomplished without mixing of the fractions by ordinary methods of pipetting. Trouble-free separation and withdrawal can, however, be obtained by the following device. Figure 11*a* shows the well-known stream line pattern about a cylindrical obstacle obtained by injecting dye on the upstream side of the cylinder. We see that the two stream lines adjacent to the vertical axis of symmetry are spread far apart as they pass the cylinder. This phenomenon can be utilized to separate and withdraw adjacent streaks of different ionic species in our apparatus as shown in Figures 11*b* and 11*c*. Figure 11*b* shows two neighboring streaks of separated ionic species streaming about the cylinder W of Figures 2, 3*a*, 3*b*, and 3*c*. The withdrawal channels O_1 and O_2 of Figure 3*b* (not labeled in Figure 11) are also

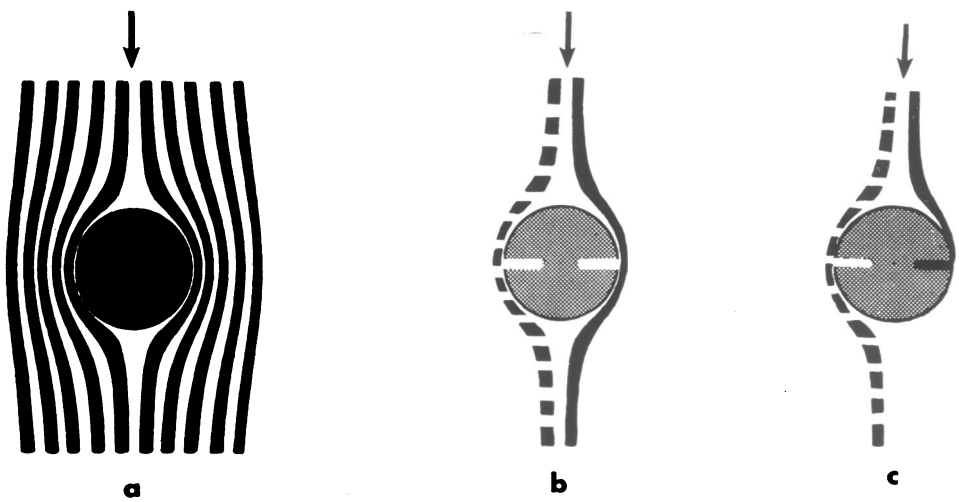

FIG. 11.—Method of separating adjacent streaks. (*a*) stream lines in flow about a cylindrical obstacle, (*b*) separation of adjacent streaks by a cylindrical obstacle, (*c*) withdrawal of a fraction (black streak). The arrows indicate the direction of streaming.

seen in Figure 11*b*. The streaks are removed from each other by the cylindrical obstacle to be withdrawn separately through the diametrically opposed openings O_1 and O_2. Figure 11*c* illustrates the withdrawal of the component shown as a black streak.

The aiming of streaks toward W so as to achieve their separation can be best accomplished by varying the magnetic field intensity. This can be done most simply by longitudinal displacement of the bar magnets. For this reason, it is advantageous not to use a perfectly uniform radial magnetic field, but, rather, an arrangement of magnets providing a section in which B_r varies slowly along the magnet axis.[14]

The method described above is very simple in operation. Its main advantages are: the use of very thin streaks which affords separation of different ionic fractions within a few seconds after traversing of a short migration path, the good stabilization against thermal convection which permits rapid fractionation through use of large potential gradients in cooled electrophoretic columns, the possibility of continuous separation, and the absence of a stabilizing medium, which makes the method suitable for studies of mobilities of suspended particles as well as of ions in solution.

The author is greatly indebted to Drs. B. Cassen and L. B. Robinson for valuable comments, to Messrs. H. S. Tillson and L. Roessner of the Research and Development Shop of the Medical School for help in the construction of the fractionation cells, and to Mr. L. B. Bright for assistance in magnetic measurements and in the preparation of the illustrations.

* This work has been supported by grants from the Office of Naval Research and from the American Cancer Society.

† Zones Z_1 and Z_2 of Figure 5 are, in our annular case, intersections of the plane of the paper with two cylindrical zones of zero velocity.

[1] Grassman, W., and K. Hannig, *Nat. Wiss.*, **37**, 93 (1950).

[2] Svensson, H., and I. Brattsten, *Arkiv Kemi*, **1**, 401 (1949).

[3] Mel, H. C., *J. Chem. Phys.*, **31**, 559 (1959).

[4] Kolin, A., *J. Chem. Phys.*, **22**, 1628 (1954).

[5] Kolin, A., these PROCEEDINGS, **41**, 101 (1955).

[6] Dobry, R., and R. K. Finn, *Science*, **127**, 697 (1958).

[7] Kolin, A., *Biochim. Biophys. Acta.*, **32**, 538 (1959).

[8] Kolin, A., *J. Appl. Phys.*, **25**, 1442 (1954).

[9] Hjertén, S., *Arkiv Kemi*, **13**, 151 (1958).

[10] Kolin, A., *Rev. Sc. Instr.*, **16**, 209(1945).

[11] Lamb, H., *Hydrodynamics* (New York: Dover, 1945), p. 582.

[12] von Smoluchowski, M., in *Handbuch der Elektrizität und des Magnetismus* (Leipzig: Barth, 1921), vol. 2, p. 366.

[13] Brinton, C. C., and M. A. Lauffer, in *Electrophoresis*, ed. M. Bier (New York: Academic Press, Inc., 1959), p. 443.

[14] As an alternative method of adjustment, *W* can be made to slide in a trough mounted over an axis-parallel slot milled on top of the outer cylinder *ET* of Figure 3*a*.